

A Chromium(III)–Superoxo Complex in Oxygen Atom Transfer Reactions as a Chemical Model of Cysteine Dioxygenase

Jaehung Cho,[§] Jaeyoung Woo,[§] and Wonwoo Nam*[§]

Department of Bioinspired Science, Ewha Womans University, Seoul 120-750, Korea

S Supporting Information

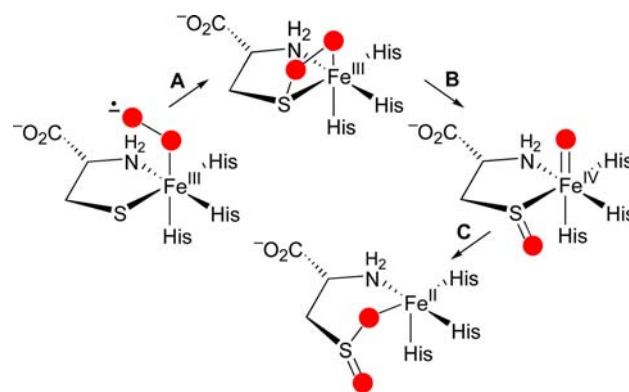
ABSTRACT: Metal–superoxo species are believed to play key roles in oxygenation reactions by metalloenzymes. One example is cysteine dioxygenase (CDO) that catalyzes the oxidation of cysteine with O₂, and an iron(III)–superoxo species is proposed as an intermediate that effects the sulfoxidation reaction. We now report the first biomimetic example showing that a chromium(III)–superoxo complex bearing a macrocyclic TMC ligand, [Cr^{III}(O₂)(TMC)(Cl)]⁺, is an active oxidant in oxygen atom transfer (OAT) reactions, such as the oxidation of phosphine and sulfides. The electrophilic character of the Cr(III)–superoxo complex is demonstrated unambiguously in the sulfoxidation of *para*-substituted thioanisoles. A Cr(IV)–oxo complex, [Cr^{IV}(O)(TMC)(Cl)]⁺, formed in the OAT reactions by the chromium(III)–superoxo complex, is characterized by X-ray crystallography and various spectroscopic methods. The present results support the proposed oxidant and mechanism in CDO, such as an iron(III)–superoxo species is an active oxidant that attacks the sulfur atom of the cysteine ligand by the terminal oxygen atom of the superoxo group, followed by the formation of a sulfoxide and an iron(IV)–oxo species via an O–O bond cleavage.

Oxygen activation at transition metal centers is of current interest in biological and catalytic oxidation reactions.¹ Oxygen-coordinating metal intermediates, such as metal–superoxo, –peroxo, –hydroperoxo, and –oxo species, are frequently invoked as plausible oxidants in the oxidation of organic substrates.¹ Among the metal–oxygen adducts, metal–superoxo species have attracted much attention recently, since the intermediates have been implicated as reactive species in the C–H bond activation of substrates by nonheme iron (e.g., isopenicillin *N* synthase and *myo*-inositol oxygenase)² and copper (e.g., dopamine β-monooxygenase and peptidylglycine-α-amidating monooxygenase)³ enzymes. In biomimetic studies, iron(III)–superoxo species have been proposed as a potent oxidant in the C–H bond activation of hydrocarbons by mononuclear nonheme iron(II) complexes.⁴ In the case of copper(II)–superoxo species, a number of synthetic copper(II)–superoxo complexes have shown reactivities in ligand oxidation and the oxidation of organic compounds with weak C–H, O–H, and N–H bonds.⁵

Cysteine dioxygenase (CDO), which is a mononuclear nonheme iron enzyme that contains an iron(II) center bound by three histidine groups in a facial orientation, catalyzes the

oxidation of cysteine with O₂ to yield cysteine sulfinic acid (i.e., *S*-oxidation).⁶ An iron(III)–superoxo intermediate is proposed as an active oxidant that attacks the sulfur atom of the ligand with the terminal oxygen atom of the superoxo group, followed by the O–O bond cleavage to form an iron(IV)–oxo species (Scheme 1).^{6,7} As a chemical model of CDO, Limberg, Goldberg, de Visser, and their co-workers reported experimental and computational studies on the iron(II)-mediated *S*-oxidation by O₂,⁸ in which iron(III)–superoxo species have been proposed as an active oxidant that effects the *S*-oxidation reactions. However, intermediacy of the iron(III)–superoxo species and the formation of an iron(IV)–oxo product in the *S*-oxidation reactions (Scheme 1) have never been observed in both enzymatic and biomimetic reactions.

Scheme 1



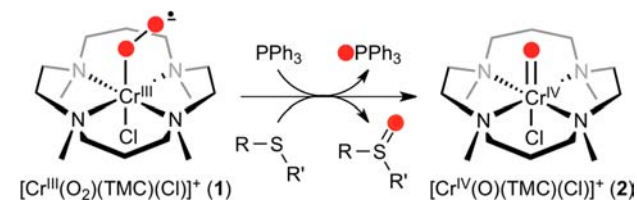
Mononuclear chromium(III)–superoxo complexes have been reported by Bakac and co-workers as chemical models of O₂ activating metalloenzymes and as active oxidants in the oxidation of substrates.⁹ Very recently, we also reported the synthesis and characterization of an end-on chromium(III)–superoxo complex, [Cr^{III}(O₂)(TMC)(Cl)]⁺ (**1**, TMC = 1,4,8,11-tetramethyl-1,4,8,11-tetraazacyclotetradecane), and highlighted its reactivity in hydrogen atom (H-atom) abstraction reactions.^{10,11} This study provided the first direct experimental evidence that metal–superoxo species are able to abstract a H-atom from external substrates. However, to the best of our knowledge, metal–superoxo complexes have never been employed in oxygen atom transfer (OAT) reactions (e.g., *S*-oxidation). In this communication, we report that **1** is able to

Received: May 5, 2012

Published: June 19, 2012

transfer its oxygen atom to organic substrates (e.g., PPh_3 and sulfides), yielding the corresponding oxygenated products and a chromium(IV)–oxo complex, $[\text{Cr}^{\text{IV}}(\text{O})(\text{TMC})(\text{Cl})]^+$ (**2**), as shown in Scheme 2. An electrophilic character of **1** is also

Scheme 2



demonstrated in the oxidation of *para*-substituted thioanisoles. Thus, the present results report a chemical model of CDO and are discussed in light of the role of an iron(III)–superoxo intermediate in the oxidation of cysteine in CDO (see Schemes 1 and 2).

The Cr(III)–superoxo complex, $[\text{Cr}^{\text{III}}(\text{O}_2)(\text{TMC})(\text{Cl})]^+$ (**1**), was generated by bubbling O_2 through a solution of $[\text{Cr}^{\text{II}}(\text{TMC})(\text{Cl})]^+$ in CH_3CN at -10°C , as reported previously.¹⁰ The intermediate **1** was metastable so that it could be used in reactivity studies under stoichiometric conditions (e.g., ca. 5% decay for 1 h at -10°C). Treating **1** with PPh_3 produced OPPh_3 in quantitative yield. The source of the oxygen incorporated into the product was determined to be the superoxo group by carrying out an isotope ^{18}O -labeling experiment; $^{18}\text{OPPh}_3$ was produced in the reaction of ^{18}O -labeled **1** ($1\text{-}^{18}\text{O}$) prepared using $^{18}\text{O}_2$ (Scheme 2; also see Supporting Information (SI), Experimental Section for reaction conditions and Figure S1). Kinetic studies of **1** with PPh_3 in CH_3CN at -10°C exhibit a first-order decay profile (Figure 1a, inset), and pseudo-first-order rate constants increased proportionally with the PPh_3 concentration, giving a second-order rate constant (k_2) of $8.4 \times 10^{-1} \text{ M}^{-1} \text{ s}^{-1}$ (Figure 1b). The rates were dependent on reaction temperature, from which a linear Eyring plot was obtained between 243 and 273 K to give the activation parameters of $\Delta H^\ddagger = 44 \text{ kJ mol}^{-1}$ and $\Delta S^\ddagger = -74 \text{ J mol}^{-1} \text{ K}^{-1}$ (Figure 1c).

We then examined the reactivity of **1** in the oxidation of sulfides in CH_3CN at -10°C . **1** disappeared upon addition of thioanisole with a first-order decay profile (Figure S2). The pseudo-first-order rate constants increased proportionally with the concentration of thioanisole ($k_2 = 5.2 \times 10^{-3} \text{ M}^{-1} \text{ s}^{-1}$) (Figure 2a).¹² The reactivity of **1** was further investigated with *para*-substituted thioanisoles, *para*-X-Ph-SCH₃ (X = OH, CH₃, H, Cl), to investigate the electronic effect of *para*-substituents on the oxidation of thioanisoles by **1** (Figure 2a). A Hammett plot of the second-order rate constants vs σ_p^+ gave a ρ value of -3.3 (Figure 2b; Table S1). Such a negative ρ value indicates the electrophilic character of the superoxo group of **1** in OAT reactions, as frequently observed in the sulfoxidation of thioanisoles by high-valent metal–oxo complexes of heme and nonheme ligands.¹³ In addition, we observed a good linear correlation when the rates were plotted against oxidation potentials (E_{ox}) of thioanisoles (Figure 2c; Table S1). Further mechanistic information needs to be obtained to clarify the mechanism of the oxygenation of sulfides by metal–superoxo species (e.g., direct oxygen atom transfer vs electron transfer followed by oxygen atom transfer).^{13,14} The product analysis of the reaction solution of the oxidation of thioanisole by **1**

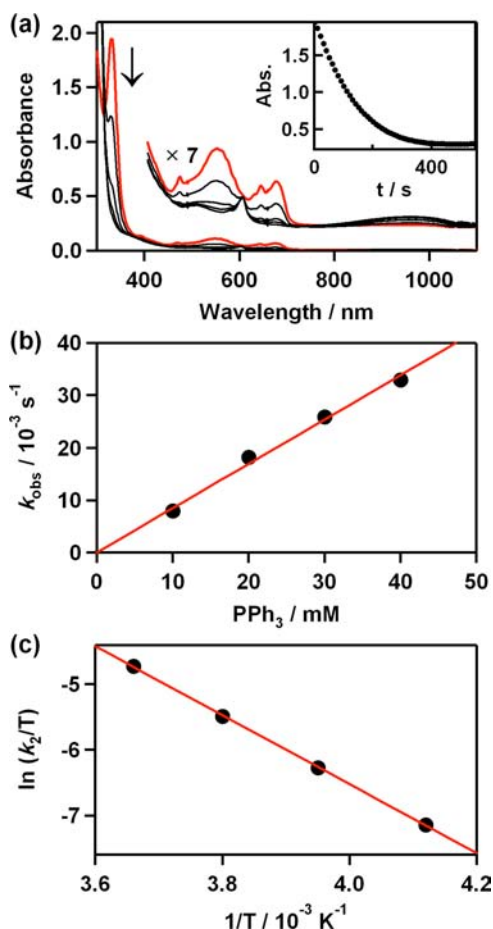


Figure 1. (a) UV–vis spectral changes of **1** (0.5 mM) obtained at 90 s intervals upon addition of PPh_3 (20 equiv to **1**, 10 mM) in CH_3CN at -10°C . The upper inset shows the time course of the decay of **1** monitored at 331 nm. The lower inset is the expanded region of 400–1100 nm ($\times 7$). (b) Plot of k_{obs} against the concentration of PPh_3 to determine a second-order rate constant at -10°C . (c) Plot of second-order rate constants against $1/T$ to determine activation parameters for the reaction of **1** and PPh_3 .

revealed that methyl phenyl sulfoxide was produced with a high yield ($\sim 70\%$ based on the amount of **1** used), and the source of oxygen in the sulfoxide product was found to be the superoxo ligand of **1** on the basis of an ^{18}O -labeling experiment performed with $1\text{-}^{18}\text{O}$ (see SI, Experimental Section for reaction conditions and Figure S3).

Interestingly, we have observed the formation of a Cr(IV)–oxo complex, $[\text{Cr}^{\text{IV}}(\text{O})(\text{TMC})(\text{Cl})]^+$ (**2**), as a product in the OAT reactions by **1** (see Scheme 2).¹⁵ This intermediate was relatively stable in CH_3CN at -10°C ($t_{1/2} \sim 40 \text{ min}$) and did not react with PPh_3 and sulfides under the conditions. Therefore, we were able to characterize **2** with various spectroscopic methods, such as UV–vis spectrophotometer, cold spray ionization mass spectrometry (CSI-MS), electron paramagnetic resonance (EPR) spectroscopy, and resonance Raman (rRaman) spectroscopy, and the structure of **2** was determined by X-ray crystallography. The UV–vis spectrum of **2** exhibits characteristic bands at 501 ($\epsilon = 60 \text{ M}^{-1} \text{ cm}^{-1}$), 603 ($\epsilon = 90 \text{ M}^{-1} \text{ cm}^{-1}$), and 960 nm ($\epsilon = 30 \text{ M}^{-1} \text{ cm}^{-1}$) (Figure 3a). The CSI-MS of **2** shows a prominent ion peak at a mass-to-charge ratio (m/z) of 359.2 (Figure 3b), whose mass and isotope distribution pattern correspond to $[\text{Cr}^{\text{IV}}(\text{O})(\text{TMC})-$

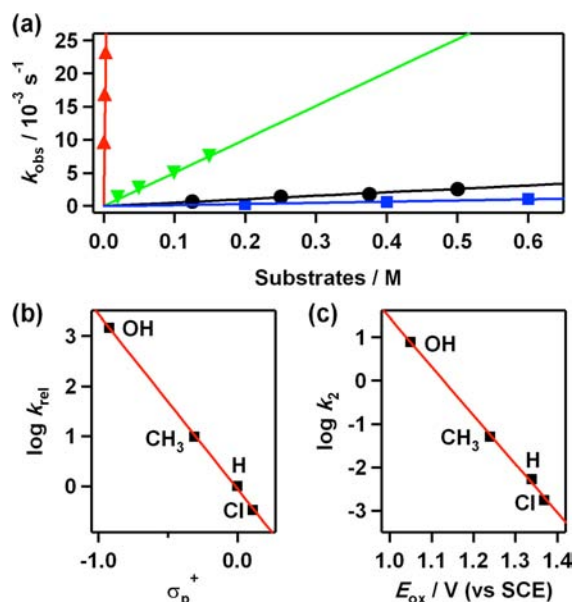


Figure 2. Reaction of **1** with *para*-substituted thioanisoles, *para*-*X*-Ph-SCH₃ (*X* = OH, CH₃, H, Cl), in CH₃CN at -10 °C. (a) Plots of k_{obs} against the concentration of *para*-*X*-Ph-SCH₃ (*X* = OH (red), CH₃ (green), H (black), Cl (blue)). (b) Hammett plot of $\log k_{\text{rel}}$ against σ_p^+ of *para*-substituted thioanisoles. The k_{rel} values were calculated by dividing k_2 of *para*-*X*-Ph-SCH₃ by k_2 of thioanisole. (c) Plot of $\log k_2$ against E_{ox} for the oxidation of *para*-substituted thioanisoles.

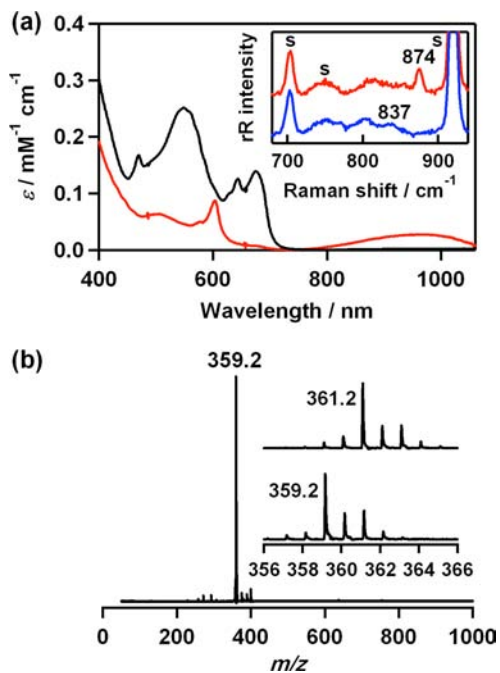


Figure 3. (a) UV-vis spectra of **2** (red line) and **1** (black line, for comparison) in CH₃CN at -10 °C. Inset shows rRaman spectra of **2**-¹⁶O (red line) and **2**-¹⁸O (blue line); solvent bands are labeled with “s”. Similar but much more intense signals were obtained for **2** which was prepared by reacting [Cr^{III}(TMC)(Cl)]⁺ with PhIO (see Figure S6). (b) CSI-MS of **2**. Inset shows isotope distribution patterns for **2**-¹⁶O (lower) and **2**-¹⁸O (upper).

(Cl)]⁺ (**2**) (calculated m/z of 359.2). When the reaction was carried out with **1**-¹⁸O (vide supra), a mass peak corresponding to [Cr^{IV}(¹⁸O)(TMC)(Cl)]⁺ (**2**-¹⁸O) appeared at a m/z of 361.2 (calculated m/z of 361.2) (Figure 3b, inset). The shift in two

mass units on substitution of ¹⁶O with ¹⁸O indicates that **2** contains one oxygen atom in it. **2** is EPR silent at 4.3 K, and the effective magnetic moment of **2** ($\mu_{\text{eff}} = 3.3 \mu_B$ at -20 °C) indicates the spin state of $S = 1$ for the Cr^{IV} ion. The rRaman spectrum of **2**-¹⁶O (32 mM), measured in CH₃CN/CH₂Cl₂ at -20 °C with 407 nm laser excitation, exhibits an isotopically sensitive band at 874 cm⁻¹, which shifted to 837 cm⁻¹ in **2**-¹⁸O (Figure 3a, inset). The observed isotopic shift of -37 cm⁻¹ with ¹⁸O-substitution is in good agreement with the calculated value ($\Delta\nu_{\text{calc}} = -38$) for the Cr–O diatomic harmonic oscillator. The observed Cr–O frequency at 873 cm⁻¹ is lower than those found in [Cr^{IV}(O)(Tp^{tBu,Me})(pzH)]⁺ (905 cm⁻¹)¹⁶ and [Cr^{IV}(O)(TPP)] (1025 cm⁻¹).¹⁷

Single crystals of **2**·Cl·CH₃CN·H₂O were grown from CH₃CN/acetone/diethyl ether at -40 °C and contained two crystallographically independent but virtually identical cations in the asymmetric unit (denoted “A” and “B”). These two cations are mononuclear chromium–oxo complexes in a distorted octahedral geometry (Tables S2 and S3), as shown in Figure 4 for **2A**. Notably, the Cr1–O1 bond length of **2A**

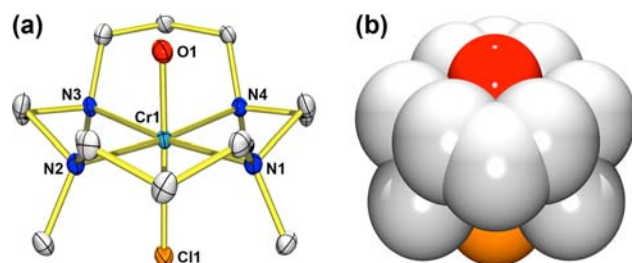


Figure 4. Molecular structure of one of crystallographically independent molecules of [Cr(O)(TMC)(Cl)]⁺ (**2**). (a) ORTEP plot of **2A** with 30% probability thermal ellipsoid. Hydrogen atoms are omitted for clarity. (b) Space-filling representation of **2A**, derived from the single crystal structure determination. Selected bond lengths (Å) and angles (°): Cr1–O1 1.698(3), Cr1–Cl1 2.3830(11), O1–Cr1–Cl1 176.82(9).

(1.698(3) Å) is longer than those of other Cr(IV or V) complexes, such as [Cr^{IV}(O)(Tp^{tBu,Me})(pzH)]⁺ (1.602 Å),¹⁶ [Cr^{IV}(O)(TPP)] (1.572 Å),¹⁷ [Cr^V(O)(salen)]⁺ (1.545 Å),¹⁸ and [Cr^V(O)(TMC)(OCH₃)₂]²⁺ (1.604 Å).¹¹ The relatively long Cr–O bond distance of **2** is consistent with the low frequency of the Cr–O stretching vibration obtained in the rRaman measurement (vide supra). In addition, intermolecular hydrogen bonding interactions in crystalline environments are proposed to elongate the Cr–O bond distance (Figure S4), as observed in Fe–O(H) complexes using the secondary coordination sphere.¹⁹ All four N-methyl groups of the TMC ligand in **2** point away from the oxo group, as observed in the crystal structures of [Cr^V(O)(TMC)(OCH₃)₂]²⁺ and [Fe^{IV}(O)(TMC)(CH₃CN)]²⁺.^{11,20}

In conclusion, we have shown recently that a Cr(III)–superoxo complex, [Cr^{III}(O₂)(TMC)(Cl)]⁺ (**1**), is a biomimetic oxidant for the metal–superoxo species proposed in C–H bond activation reactions by nonheme iron and copper enzymes. In the present study, we have demonstrated that **1** is able to conduct OAT reactions with an electrophilic character. We have also shown the formation of a chromium(IV)–oxo complex, [Cr^{IV}(O)(TMC)(Cl)]⁺ (**2**), in the OAT reactions by **1**. Thus, the present study provides the first biomimetic example demonstrating that a metal(III)–superoxo complex possesses an electrophilic character and is able to conduct OAT

reactions. In addition, a metal(IV)–oxo complex is formed as a product when the terminal oxygen atom of the superoxo group in the metal(III)–superoxo complex is transferred to organic substrates in the OAT reactions (see Schemes 1 and 2). Further studies, including density functional theory (DFT) calculations, will provide insights regarding the mechanism of the oxygen atom transfer from metal–superoxo species to organic substrates in enzymatic and biomimetic reactions.

■ ASSOCIATED CONTENT

■ Supporting Information

Experimental Section, Tables S1–S3, and Figures S1–S6. This material is available free of charge via the Internet at <http://pubs.acs.org>.

■ AUTHOR INFORMATION

Corresponding Author

wwnam@ewha.ac.kr

Author Contributions

[§]These authors contributed equally.

Notes

The authors declare no competing financial interest.

■ ACKNOWLEDGMENTS

The research was supported by KRF/MEST of Korea through CRI, GRL (2010-00353), and WCU (R31-2008-000-10010-0) (to W.N.). We thank Prof. Takashi Ogura and Takashi Nomura of University of Hyogo for their help in the measurement of resonance Raman spectra.

■ REFERENCES

- (1) (a) Ortiz de Montellano, P. R. *Chem. Rev.* **2010**, *110*, 932–948. (b) Green, M. T. *Curr. Opin. Chem. Biol.* **2009**, *13*, 84–88. (c) Krebs, C.; Fujimori, D. G.; Walsh, C. T.; Bollinger, J. M., Jr. *Acc. Chem. Res.* **2007**, *40*, 484–492. (d) Nam, W. *Acc. Chem. Res.* **2007**, *40*, 465 and review articles in the special issue. (e) Abu-Omar, M. M.; Loaiza, A.; Hontzeas, N. *Chem. Rev.* **2005**, *105*, 2227–2252. (f) Klotz, I. M.; Kurtz, D. M., Jr. *Chem. Rev.* **1994**, *94*, 567–568 and review articles in the special issue.
- (2) (a) Bollinger, J. M., Jr.; Krebs, C. *Curr. Opin. Chem. Biol.* **2007**, *11*, 151–158. (b) van der Donk, W. A.; Krebs, C.; Bollinger, J. M., Jr. *Curr. Opin. Struct. Biol.* **2010**, *20*, 673–683.
- (3) (a) Prigge, S. T.; Eipper, B. A.; Mains, R. E.; Amzel, L. M. *Science* **2004**, *304*, 864–867. (b) Chen, P.; Solomon, E. I. *Proc. Natl. Acad. Sci. U.S.A.* **2004**, *101*, 13105–13110. (c) Klinman, J. P. *J. Biol. Chem.* **2006**, *281*, 3013–3016. (d) Rolff, M.; Tuzcek, F. *Angew. Chem., Int. Ed.* **2008**, *47*, 2344–2347.
- (4) (a) Lee, Y.-M.; Hong, S.; Morimoto, Y.; Shin, W.; Fukuzumi, S.; Nam, W. *J. Am. Chem. Soc.* **2010**, *132*, 10668–10670. (b) Mukherjee, A.; Cranswick, M. A.; Chakrabarti, M.; Paine, T. K.; Fujisawa, K.; Münck, E.; Que, L., Jr. *Inorg. Chem.* **2010**, *49*, 3618–3628. (c) Chen, H.; Cho, K.-B.; Lai, W.; Nam, W.; Shaik, S. *J. Chem. Theory Comput.* **2012**, *8*, 915–926. (d) Chung, L. W.; Li, X.; Hirao, H.; Morokuma, K. *J. Am. Chem. Soc.* **2011**, *133*, 20076–20079.
- (5) (a) Peterson, R. L.; Himes, R. A.; Kotani, H.; Suenobu, T.; Tian, L.; Siegler, M. A.; Solomon, E. I.; Fukuzumi, S.; Karlin, K. D. *J. Am. Chem. Soc.* **2011**, *133*, 1702–1705. (b) Kunishita, A.; Kubo, M.; Sugimoto, H.; Ogura, T.; Sato, K.; Takui, T.; Itoh, S. *J. Am. Chem. Soc.* **2009**, *131*, 2788–2789. (c) Maiti, D.; Lee, D.-H.; Gaoutchenova, K.; Würtele, C.; Holthausen, M. C.; Narducci Sarjeant, A. A.; Sundermeyer, J.; Schindler, S.; Karlin, K. D. *Angew. Chem., Int. Ed.* **2008**, *47*, 82–85. (d) Maiti, D.; Fry, H. C.; Woertink, J. S.; Vance, M. A.; Solomon, E. I.; Karlin, K. D. *J. Am. Chem. Soc.* **2007**, *129*, 264–265. (e) Cramer, C. J.; Tolman, W. B. *Acc. Chem. Res.* **2007**, *40*, 601–608. (f) Würtele, C.; Gaoutchenova, E.; Harms, K.; Holthausen, M. C.; Sundermeyer, J.; Schindler, S. *Angew. Chem., Int. Ed.* **2006**, *45*, 3867–3869. (g) Itoh, S. *Curr. Opin. Chem. Biol.* **2006**, *10*, 115–122.
- (6) (a) McCoy, J. G.; Bailey, L. J.; Bitto, E.; Bingman, C. A.; Aceti, D. J.; Fox, B. G.; Phillips, G. N., Jr. *Proc. Natl. Acad. Sci. U.S.A.* **2006**, *103*, 3084–3089. (b) Joseph, C. A.; Maroney, M. J. *Chem. Commun.* **2007**, 3338–3349. (c) de Visser, S. P.; Straganz, G. D. *J. Phys. Chem. A* **2009**, *113*, 1835–1846. (d) de Visser, S. P. *Coord. Chem. Rev.* **2009**, *253*, 754–768.
- (7) (a) Crawford, J. A.; Li, W.; Pierce, B. S. *Biochemistry* **2011**, *50*, 10241–10253. (b) Kumar, D.; Thiel, W.; de Visser, S. P. *J. Am. Chem. Soc.* **2011**, *133*, 3869–3882. (c) Pierce, B. S.; Gardner, J. D.; Bailey, L. J.; Brunold, T. C.; Fox, B. G. *Biochemistry* **2007**, *46*, 8569–8578. (d) Aluri, S.; de Visser, S. P. *J. Am. Chem. Soc.* **2007**, *129*, 14846–14847.
- (8) (a) Sallmann, M.; Siewert, I.; Fohlmeister, L.; Limberg, C.; Knispel, C. *Angew. Chem., Int. Ed.* **2012**, *51*, 2234–2237. (b) Badiei, Y. M.; Siegler, M. A.; Goldberg, D. P. *J. Am. Chem. Soc.* **2011**, *133*, 1274–1277. (c) Kumar, D.; Sastry, G. N.; Goldberg, D. P.; de Visser, S. P. *J. Phys. Chem. A* **2012**, *116*, 582–591. (d) Jiang, Y.; Widger, L. R.; Kasper, G. D.; Siegler, M. A.; Goldberg, D. P. *J. Am. Chem. Soc.* **2010**, *132*, 12214–12215. (e) McQuilken, A. C.; Jiang, Y.; Siegler, M. A.; Goldberg, D. P. *J. Am. Chem. Soc.* **2012**, *134*, 8758–8761.
- (9) (a) Bakac, A.; Scott, S. L.; Espenson, J. H.; Rodgers, K. R. *J. Am. Chem. Soc.* **1995**, *117*, 6483–6488. (b) Bakac, A. *J. Am. Chem. Soc.* **1997**, *119*, 10726–10731. (c) Bakac, A. *Coord. Chem. Rev.* **2006**, *250*, 2046–2058.
- (10) Cho, J.; Woo, J.; Nam, W. *J. Am. Chem. Soc.* **2010**, *132*, 5958–5959.
- (11) Cho, J.; Woo, J.; Han, J. E.; Kubo, M.; Ogura, T.; Nam, W. *Chem. Sci.* **2011**, *2*, 2057–2062.
- (12) We have reported the hydrogen atom transfer (HAT) reactivity of **1** in the C–H bond activation of substrates with weak bond dissociation energies such as 9,10-dihydroanthracene ($k_2 = 1.7 \times 10^{-1} \text{ M}^{-1} \text{ s}^{-1}$ at -10°C) in ref 10. By comparing the rate of the oxidation of thioanisole by **1** ($k_2 = 5.2 \times 10^{-3} \text{ M}^{-1} \text{ s}^{-1}$ at -10°C) to that of the HAT reaction, we found that the HAT reaction is faster than the OAT reaction.
- (13) (a) Arias, J.; Newlands, C. R.; Abu-Omar, M. M. *Inorg. Chem.* **2001**, *40*, 2185–2192. (b) McPherson, L. D.; Drees, M.; Khan, S. I.; Strassner, T.; Abu-Omar, M. M. *Inorg. Chem.* **2004**, *43*, 4036–4050. (c) Sastri, C. V.; Seo, M. S.; Park, M. J.; Kim, K. M.; Nam, W. *Chem. Commun.* **2005**, 1405–1407. (d) Nam, W. *Acc. Chem. Res.* **2007**, *40*, 522–531.
- (14) (a) Goto, Y.; Matsui, T.; Ozaki, S.; Watanabe, Y.; Fukuzumi, S. *J. Am. Chem. Soc.* **1999**, *121*, 9497–9502. (b) Taki, M.; Itoh, S.; Fukuzumi, S. *J. Am. Chem. Soc.* **2002**, *124*, 998–1002. (c) Kumar, A.; Goldberg, I.; Botoshansky, M.; Buchman, Y.; Gross, Z. *J. Am. Chem. Soc.* **2010**, *132*, 15233–15245. (d) Park, J.; Morimoto, Y.; Lee, Y.-M.; Nam, W.; Fukuzumi, S. *J. Am. Chem. Soc.* **2011**, *133*, 5236–5239.
- (15) **2** was synthesized independently by reacting $[\text{Cr}^{\text{II}}(\text{TMC})(\text{Cl})]^+$ with 3.6 equiv of iodobenzene (PhIO) in CH_3CN at -10°C , although this reaction afforded ca. 60% formation of **2** based on the UV–vis spectrum (Figure S5), and this species was further characterized with resonance Raman spectroscopy (Figure S6).
- (16) Qin, K.; Incarvito, C. D.; Rheingold, A. L.; Theopold, K. H. *J. Am. Chem. Soc.* **2002**, *124*, 14008–14009.
- (17) Groves, J. T.; Kruper, W. J., Jr.; Haushalter, R. C.; Butler, W. M. *Inorg. Chem.* **1982**, *21*, 1363–1368.
- (18) Srinivasan, K.; Kochi, J. K. *Inorg. Chem.* **1985**, *24*, 4671–4679.
- (19) (a) Shook, R. L.; Borovik, A. S. *Chem. Commun.* **2008**, 6095–6107. (b) Mukherjee, J.; Lucas, R. L.; Zart, M. K.; Powell, D. R.; Day, V. W.; Borovik, A. S. *Inorg. Chem.* **2008**, *47*, 5780–5786. (c) Conradie, J.; Tangen, E.; Ghosh, A. *J. Inorg. Biochem.* **2006**, *100*, 707–715.
- (20) Rohde, J.-U.; In, J.-H.; Lim, M. H.; Brennessel, W. W.; Bukowski, M. R.; Stubna, A.; Münck, E.; Nam, W.; Que, L., Jr. *Science* **2003**, *229*, 1037–1039.